Dopamine dynamics and cocaine sensitivity differ between striosome and matrix compartments of the striatum

Armando G. Salinas[a,b], **Margaret I. Davis**[b], **David M. Lovinger**[b], and **Yolanda Mateo**[b,*]

[a]The Krasnow Institute for Advanced Study, George Mason University, Fairfax, VA 22030, USA

[b]Laboratory for Integrative Neuroscience, Section on Synaptic Pharmacology, National Institute on Alcohol Abuse and Alcoholism, Rockville, MD 20852, USA

Abstract

The striatum is typically classified according to its major output pathways, which consist of dopamine D1 and D2 receptor-expressing neurons. The striatum is also divided into striosome and matrix compartments, based on the differential expression of a number of proteins, including the mu opioid receptor, dopamine transporter (DAT), and Nr4a1 (nuclear receptor subfamily 4, group A, member 1). Numerous functional differences between the striosome and matrix compartments are implicated in dopamine-related neurological disorders including Parkinson's disease and addiction. Using Nr4a1-eGFP mice, we provide evidence that electrically evoked dopamine release differs between the striosome and matrix compartments in a regionally-distinct manner. We further demonstrate that this difference is not due to differences in inhibition of dopamine release by dopamine autoreceptors or nicotinic acetylcholine receptors. Furthermore, cocaine enhanced extracellular dopamine in striosomes to a greater degree than in the matrix and concomitantly inhibited dopamine uptake in the matrix to a greater degree than in striosomes. Importantly, these compartment differences in cocaine sensitivity were limited to the dorsal striatum. These findings demonstrate a level of exquisite microanatomical regulation of dopamine by the DAT in striosomes relative to the matrix.

1. Introduction

The striatum has been characterized according to its two major output pathways: the direct pathway (dopamine D1 receptor-expressing neurons) and the indirect pathway (dopamine D2 receptor-expressing neurons) (Gerfen et al., 1990). The striatum can also be classified into two neurochemically-distinct compartments, the striosome and matrix, based on the

differential expression of several proteins, including the mu opioid receptor (MOR), acetyl-cholinesterase, dopamine transporter (DAT), and Nr4a1 (nuclear receptor subfamily 4, group A, member 1) (Crittenden and Graybiel, 2011; Davis and Puhl, 2011; Graybiel and Ragsdale, 1978; Herkenham and Pert, 1981). The matrix compartment comprises approximately 85% of the striatum (Johnston et al., 1990; Mikula et al., 2009) and functions as part of the sensorimotor and associative circuits; in contrast, the striosome compartment comprises approximately 15% of the striatum and is associated with limbic circuits (Eblen and Graybiel, 1995; Gerfen, 1984; Jimenez-Castellanos and Graybiel, 1987; Kincaid and Wilson, 1996). However, these ratios vary across the rostrocaudal extent of the striatum (Davis and Puhl, 2011). Striosome projection neurons are primarily direct pathway neurons developmentally, while matrix projection neurons are either direct or indirect pathway (Fujiyama et al., 2011), though some controversy remains and may be attributable to species differences (Levesque and Parent, 2005). Interestingly, it is theorized that only striatal projection neurons originating in striosomes innervate the substantia nigra pars compacta (SNc) and in this way may globally influence dopamine release in the striatum (Fujiyama et al., 2011; Gerfen et al., 1987; Watabe-Uchida et al., 2012).

Midbrain dopaminergic innervation of the striatum follows a topographical pattern where the dorsal striatum (DS) is innervated primarily by the substantia nigra (and to a lesser extent the lateral ventral tegmental area) and the ventral striatum (VS) is innervated primarily by the ventral tegmental area (VTA) (Beier et al., 2015; Ikemoto, 2007; Lammel et al., 2008). The dopaminergic innervation of the matrix compartment reflects this topographical pattern, but striosomal dopamine originates largely from the SNc and to a lesser extent the substantia nigra pars reticulata (Gerfen et al., 1987; Jimenez-Castellanos and Graybiel, 1987; Langer and Graybiel, 1989; Prensa and Parent, 2001). Related to these differences in compartmental dopamine innervation, numerous animal models of Parkinson's disease and dystonia show preferential loss of dopamine terminals or striatal projection neurons in either the striosome or matrix compartments (see Crittenden and Graybiel (2011) for review). Similarly, imbalances in chronic drug-induced immediate early gene expression between striosome and matrix compartments underlie psychostimulant-induced stereotypies (Canales and Graybiel, 2000; Capper-Loup et al., 2002; Jedynak et al., 2012). Given the differences in compartmental dopamine origin and the putative roles of striosome and matrix compartments in numerous dopamine-related neurological disorders, we hypothesized that dopamine signaling between striatal compartments would differ.

Nr4a1 (also known as Nur77 and NGFIB; Entrez Gene ID: 15370) is a nuclear receptor protein initially identified in silico by Davis and Puhl (2011) as a marker for striosomes. Therefore, in the current study, we used fast-scan cyclic voltammetry (FSCV) and Nr4a1-eGFP transgenic mice to identify striosomes and to directly compare dopamine release between the striosome and matrix compartments of the striatum. We found that electrically evoked dopamine release differed between striosome and matrix compartments in a region-specific manner and that these differences could not be attributed to nicotinic acetylcholine receptor (nAChR) antagonism or dopamine D2 autoreceptor inhibition of the dopamine terminal. We further found that cocaine-enhanced dopamine levels and uptake inhibition differed between striosome and matrix compartments in the dorsal, but not ventral, striatum.

These findings demonstrate a previously undescribed compartment difference in cocaine mediated regulation of dopamine dynamics in the striatum.

2. Methods

2.1. Subjects

Nr4a1-eGFP mice were obtained from GENSAT and backcrossed with C57BL6J mice (The Jackson Laboratory) for at least six generations. At weaning, visual genotyping with a blue LED and GFP filter-equipped goggles (Electron Microscopy Sciences) was performed. $Drd2^{loxp/loxp}$ mice were obtained from The Jackson Laboratory and crossed with Adora2A-Cre mice (KG139, GENSAT). The A2ACre/$Drd2^{loxp}$ pups were then crossed with $Drd2^{loxp/loxp}$ mice to generate A2ACre/$Drd2^{loxp/loxp}$ (KO) and $Drd2^{loxp/loxp}$ mice (WT). Two to five month old mice of both sexes were used for all experiments. All experimental procedures were approved by the National Institute on Alcohol Abuse and Alcoholism Animal Care and Use Committee and were performed in accordance with National Institutes of Health guidelines.

2.2. Immunofluorescence

Mice were anesthetized with pentobarbital and transcardially perfused with a 4% formaldehyde/PBS solution. The brains were then extracted and post-fixed overnight before being stored in PBS for later sectioning. Forty micron thick sections were blocked in a 5% bovine serum albumin, 0.2% Triton X-100, PBS solution for 4 h at room temperature. The sections were then incubated in a primary antibody/PBS solution overnight as follows: chicken anti-GFP (1/ 2000; Abcam, ab13970), rabbit anti-MOR (1/4000; Immunostar, 24216), rabbit anti-D2DR (1/500; Frontier Institute, D2R-Rb-Af750), and rat anti-DAT (1/5000; Millipore, MAB369). Sections were then washed three times in 0.2% Triton X-100/PBS before being incubated in secondary antibody solutions with Alexa488 goat anti-chicken (1/2000), Alexa568 goat anti-rabbit (1/1000), or Alexa568 goat anti-rat (1/1000) overnight (secondary antibodies were from Life Technologies). Following five washes in PBS, sections were mounted onto subbed slides, coverslipped with Fluoromount G (Electron Microscopy Sciences), and imaged with a Zeiss Lumar stereoscope and an Axiovert 200 microscope equipped with DAPI, eGFP, and Cy3 filter sets and an Axiocam MR fluorescence camera with Axiovision software (Zeiss).

2.3. Ex vivo slice preparation and fast-scan cyclic voltammetry

Mice were anesthetized with isoflurane and rapidly decapitated. Brains were extracted and immersed in ice-cold, carbogen-saturated (95% O_2/5% CO_2), cutting ACSF containing the following (in mM): Sucrose (194), NaCl (30), KCl (4.5), $NaHCO_3$ (26), NaH_2PO_4 (1.2), dextrose (10), and $MgCl_2$ (1). Coronal sections (300 μm) spanning the striatum were prepared as previously described (John and Jones, 2007) and incubated for 1 h before experiments in carbogen-saturated voltammetry recording ACSF (pH 7.4) containing (in mM): NaCl (126), KCl (2.5), $NaHCO_3$ (25), NaH_2PO_4 (1.2), dextrose (10), HEPES (20), $CaCl_2$ (2.4), $MgCl_2$ (1.2), and L-ascorbic acid (0.4). Nr4a1-eGFP fluorescence was observed using a Stereo-Discovery V8 microscope with a GFP filter set (Zeiss) and an X-cite 120 fluorescence illuminator (Lumen Dynamics). One millisecond, monophasic electrical pulses

were generated with a DS3 Constant Current Stimulator (Digitimer) and delivered through a twisted, bipolar, stainless steel stimulating electrode (Plastics One) placed 300 μm from the intended recording sites as shown in Fig. 2A. The distance between the two poles of the stimulating electrode was adjusted to 250 μm.

Carbon fiber electrodes were made as previously described (Crowley et al., 2014) and cut to 80–120 μm. The carbon fiber electrode potential was linearly scanned as a triangle waveform from −0.4 to 1.2 and back to −0.4 V at 400 V/s. Cyclic voltammograms were collected at 10 Hz using a Chem-Clamp (Dagan Corporation) and DEMON Voltammetry and Analysis software (Yorgason et al., 2011). Dopamine release was evoked by single electrical stimulations delivered every 3 min (5 min for cocaine experiments). For experiments comparing dopamine release between compartments, the carbon fiber was placed in the matrix or striosome compartment 300 μm from the stimulating electrode. The stimulation intensity used for each experiment was selected to yield a transient peak approximately 40%–60% of the maximum transient peak (as determined from a preliminary input-output curve for each slice once stable transients were obtained but before baseline measurements) and ranged from 100 to 300 μA. Once five consecutive stable responses were collected (<10% variation in transient peak), experiments would begin. Four to five baseline measurements in the first compartment were collected and then the carbon fiber electrode was moved to the complementary compartment at the same distance from the stimulating electrode. Another four or five responses were collected in the second compartment at the same stimulation intensity as the first compartment. The order of starting compartment was counterbalanced between slices for all experiments. Dopamine transient decay rates, tau, were calculated from an exponential fit encompassing the dopamine transient peak and return to baseline with the data analysis module in DEMON. For experiments examining drug effects between compartments, data were normalized to their respective baseline/pre-drug periods. For modeling of dopamine transient kinetics (V_{max} and apparent K_m) in the cocaine experiments, a Michaelis-Menten-based kinetic modeling module (based on Wu et al. (2001)) in DEMON was used. Briefly, dopamine release [DAp] and dopamine affinity for the transporter (K_m; set to 0.16 μM) were held constant for the baseline determination of maximal uptake rates (V_{max}) for each experiment. Then following cocaine wash on, the obtained V_{max} for each slice was held constant and K_m was varied to fit the empirically obtained dopamine transients. The resultant K_m value reflects the affinity of dopamine for the transporter in the presence of cocaine (i.e. the apparent K_m). Extracellular dopamine concentrations were determined by post hoc calibrations against a 1 μM dopamine solution.

2.4. Drugs

Dopamine-HCl was obtained from Sigma Aldrich (St. Louis, MO). Quinpirole (30 nM) and DHβE (1 μM) were obtained from Tocris Bioscience (Minneapolis, MN). Cocaine-HCl (0.3–10 μM) was obtained from the National Institute on Drug Abuse (NIDA). All drugs were dissolved in voltammetry recording ACSF.

2.5. Statistics

GraphPad Prism 6 (GraphPad Software) was used for all statistics. Unpaired t-tests were used for the experiments examining dopamine release and dopamine transient decay rates

(Tau) between compartments. For experiments in Figs. 3 and 4, the final drug time points were analyzed with a two-factor ANOVA (region and compartment). For cocaine experiments, two-factor, repeated-measures ANOVAs were used.

3. Results

3.1. Nr4a1-eGFP is enhanced in striosomes and colocalizes with DAT

Nr4a1-eGFP was expressed throughout the striatum as previously described (Davis and Puhl, 2011) and colocalized extensively with immunoreactivity for the MOR, a striosomal marker (Fig. 1A and B). We also examined the colocalization of Nr4a1-eGFP with DAT throughout the striatum. We observed extensive colocalization of Nr4a1 with DAT in the DS. The degree of colocalization in the VS, however, was negligible (Fig. 1B).

3.2. Evoked dopamine release differs between striosome and matrix compartments

We employed FSCV to directly compare dopamine release between striatal compartments. In the DS (medial and lateral), we found that evoked dopamine release in striosomes was approximately 36% lower than in the corresponding proximal matrix region (n = 16 slices, t(30) = 2.92, p < 0.007; Fig. 2C and E). Representative color plots are shown are shown in 2D. In the VS (ventral lateral striatum and nucleus accumbens), this pattern was reversed such that evoked dopamine release in striosomes was 64% greater than in the proximal matrix region (n = 14 slices, t(26) = 2.34, p < 0.03; Fig. 2H and J). Representative color plots are shown are shown in 2I. The dopamine transient decay rates (Tau) were similar between compartments (n = 16 slices, t(30) = 0.89, p > 0.3 and n = 14 slices, t(26) = 0.76, p > 0.4, respectively for DS and VS; Fig. 2F and K). The compartment differences in dopamine release persisted across multiple stimulation intensities in both the dorsal (Fig. 2G) and ventral striatum (Fig. 2L). There were main effects of both compartment and stimulation intensity, as well as, an interaction effect in the dorsal striatum (n = 4 slices; F(1,6) = 12.22, p < 0.02 for compartment; F(4,24) = 27.97, p < 0.001 for stimulation intensity; F(4,24) = 7.08, p < 0.001 for interaction effect). In the ventral striatum we found main effects of compartment and stimulation intensity (n = 5 slices, F(1,8) = 6.3, p < 0.04 and F(4,32) = 28.23, p < 0.001, respectively for compartment and stimulation intensity).

3.3. Modulation of dopamine release dopamine D2 receptors is similar between compartments

To account for the compartment differences in dopamine release, we first examined the role of dopamine D2 autoreceptors with the dopamine D2 receptor agonist, quinpirole. Activation of dopamine D2 receptors (including autoreceptors on dopamine terminals) depressed dopamine release in both compartments across striatal regions (n = 3 slices per group, F(1,8) = 48.84, p < 0.001 and F(1,8) = 52.35, p < 0.001, respectively for the dorsal and ventral striatum; Fig. 3A). We observed a striosomal enrichment of D2DR immunoreactivity (Fig. 3B), however, the results with stimulated dopamine release did not indicate any functional difference in receptors between compartments. We considered the possibility that the D2DR striosomal enrichment was not due to differences in D2DR expression on dopamine terminals, but to differences in D2DR expression on MSNs. To test this hypothesis, we used a transgenic mouse expressing Cre recombinase in D2DR

expressing MSNs (i.e. A2ACre mice) and crossed it with a mouse line of Drd2[loxp/loxp] mice to remove D2DRs from all MSNs expressing Cre recombinase (i.e. indirect pathway/D2DR and A2AR-expressing MSNs). Subsequent histochemical examination of D2DR immunoreactivity in the Drd2[loxp/loxp] mice revealed a striosomal enrichment of DRD2s that was lost in A2ACre-Drd2[loxp/loxp] mice, suggesting that the observed striosomal enrichment of DRD2s was largely due to MSN-MSN collaterals and not presynaptic autoreceptors (Fig. 3B). Finally, we repeated our initial experiments directly examining compartment differences in dopamine release in the presence of 30 nM quinpirole and found that the compartment differences were unaffected by quinpirole (Fig. 3C and D, n = 5 slices, $t(8)$ = 2.862, $p < 0.03$ and Fig. 3E and F, n = 4 slices, $t(6)$ = 3.296, $p < 0.02$, for the dorsal and ventral striatum, respectively).

3.4. Compartment differences in dopamine release are not due to nAChRs

Cholinergic transmission via nAChRs has recently been demonstrated to influence dopamine transmission (Cachope et al., 2012; Threlfell et al., 2012), therefore, we examined the potential role of nAChRs in our observed compartment differences in dopamine transmission. Antagonism of β2-containing nAChRs depressed dopamine release in both compartments in the DS and VS (n = 4–5 slices per group, $F(1,14)$ = 1136, $p < 0.001$ and $F(1,16)$ = 1062, $p < 0.001$, respectively for dorsal and ventral striatum; Fig. 4A). We further found that our observed compartment differences persisted in the presence of DHβE in both the dorsal (Fig. 4B and C) and ventral (Fig. 4D and E) striatum, suggesting that nAChRs are not the mediators of the compartment differences in dopamine transmission.

3.5. Dopamine transporter inhibition by cocaine differs between the striosome and matrix compartments

Given the enhanced striosomal expression of DAT, we next investigated the DAT contribution to evoked dopamine levels with the DAT inhibitor, cocaine. The cocaine effect on evoked dopamine release followed a classic inverted U concentration response curve in striosome and matrix compartments of both dorsal and ventral striatal regions (Fig. 5). At concentrations up to 3 μM, cocaine enhanced dopamine spillover in both compartments. Following application of 10 μM cocaine, however, evoked dopamine release was inhibited (Fig. 5A and D), presumably due to nonspecific concentration-dependent cocaine inhibition of nAChRs (Acevedo-Rodriguez et al., 2014). In the DS there were main effects of compartment and cocaine concentration (n = 4–5 slices per group, $F(1,35)$ = 15.73, $p < 0.001$ and $F(4,35)$ = 19.71, $p < 0.001$, respectively for compartment and concentration; Fig. 5A) on cocaine-enhanced stimulation-induced dopamine release. Michaelis-Menten modeling of dopamine kinetics revealed no significant compartment differences in maximal dopamine uptake (V_{max}, n = 4–5 slices per group, $t(7)$ = 0.92, $p > 0.3$; Fig. 5B); however, apparent K_m, the observed affinity of dopamine for the transporter, was increased to a greater degree in the matrix than in striosomes (n = 4–5 slices per group, $F(1,35)$ = 7.119, $p < 0.02$; Fig. 5C) indicating a lower dopamine uptake rate or increased dopamine uptake inhibition. In the VS, there was a main effect of cocaine concentration on evoked dopamine levels (n = 3–4 slices per group, $F(4,25)$ = 16.49, $p < 0.001$; Fig. 5D), but no significant difference in dopamine signals between compartments ($F(1,25)$ = 2.395, $p > 0.1$). V_{max} and apparent K_m, also failed to show compartment differences in the VS (n = 3–4 slices per

group, t(5) = 0.02, p > 0.9 and n = 3–4 slices per group, $F(1,25) < 0.0001$, p > 0.9, for V_{max} and apparent K_m, respectively; Fig. 5E and F).

4. Discussion

We found that dopamine release differed between striosome and matrix compartments of the striatum in a regionally-distinct manner such that in the DS, dopamine release in striosomes was less than in the matrix, and in the VS, the opposite was true. We also found that cocaine differentially affects dopamine dynamics between striosome and matrix compartments. Specifically, cocaine enhanced dopamine overflow to a greater degree in striosomes than in proximal matrix regions. Concurrently, cocaine increased apparent K_m, reflecting a greater inhibition of the DAT, in the matrix to a greater degree than in striosomes; however, these DAT effects were limited to the DS.

To account for the observed compartment differences in dopa-mine release, we first considered technical aspects of our preparation. In particular, we considered whether the electrical stimulation site could differentially impact dopamine release between compartments; however, because of the large stimulating electrode, we believe that the stimulation field was not limited to any one compartment and therefore was not a factor in our observed compartmental differences. Furthermore, given the limited sampling area/volume of carbon fiber electrodes (Cragg and Rice, 2004), the only dopamine detected likely originated from synapses within the compartment being sampled. Finally, we examined whether our observed compartment differences would persist across various stimulation intensities and, indeed, found that the compartment differences in both the dorsal and ventral striatum were not unique to a particular stimulation intensity. Therefore, we do not believe that there are compartment-specific stimulation effects on dopamine release. Recently, however, a disynaptic mechanism of dopamine release has been described with electrical stimulation (Cachope et al., 2012; Threlfell et al., 2012). In this mechanism, electrical stimulation elicits dopamine release both by direct depolarization of the dopamine terminal as well as depolarization of acetylcholine terminals. To rule out the possibility of a disynaptic mechanism underlying our compartment differences, we investigated the potential role of nAChRs, which have been shown to contribute to dopamine release (Cachope et al., 2012; Rice and Cragg, 2004; Threlfell et al., 2012; Zhang et al., 2009b), and found that the antagonism of nAChRs with DHβE had a comparable effect on dopamine release in both compartments (Kemel et al., 1989, 1992). Further supporting these findings, we reassessed the compartment differences in dopamine transmission in the presence of DHβE and found that the compartment differences persisted in both the dorsal and ventral striatum. Thus, we believe the differences we observed are due to the direct depolarizing effects of electrical stimulation on dopamine terminals only, and not to any indirect dopamine release mechanisms (e.g. via cholinergic interneurons). We then assessed dopamine D2 autoreceptor modulation between compartments with the D2DR agonist, quinpirole. Despite compartment differences in the expression of D2DRs, we found that quinpirole inhibited dopamine release similarly between compartments and that the compartment differences in dopamine release persisted in the presence of D2DR agonism with quinpirole. However, a subsequent analysis of D2DR-ir in A2A-Cre:D2DR[loxp/loxp] (i.e. mice with D2DR removed from indirect pathway/D2DR-expressing MSNs) and control mice revealed that the

striosomal enrichment of D2DR was due to increased expression on MSN-MSN collaterals and not to compartment differences in expression on dopamine terminals. Thus, our voltammetry data concerning the ability of D2 autoreceptors to inhibit dopamine release between compartments is in accord with our neuroanatomical data. We then examined the effect of cocaine on evoked dopamine release and found that cocaine enhanced peak dopamine signals in striosomes to a greater degree than in the matrix and inhibited the DAT to a greater degree in the matrix than in striosomes. These differences in cocaine sensitivity were limited to the DS; therefore, it is unlikely that differences in DAT underlie all of the differences in dopamine release across striatal regions. Interestingly, we noted no differences in basal dopamine transient decay rates (tau) or in basal V_{max}, suggesting that under basal conditions the contribution of DAT is similar between compartments. In the presence of cocaine, however, both release and K_m were differentially affected. It is possible that cocaine can differentially recruit dopamine vesicle reserve pools between compartments, which might suggest compartment differences in vesicle release mechanisms, though this possibility would need to be further explored (Venton et al., 2006).

Another potential mechanism underlying the compartment differences in dopamine release is the source of dopamine. Striosomes across the striatum are largely innervated by dopamine from the SNc, while the matrix receives dopamine from the substantia nigra in the DS and the VTA in the VS (Gerfen et al., 1987; Ikemoto, 2007; Jimenez-Castellanos and Graybiel, 1987; Lammel et al., 2008; Langer and Graybiel, 1989; Prensa and Parent, 2001). It is possible that the amount of dopamine released in striosomes is similar in the DS and VS, but the amount of dopamine released in the matrix varies across the dorsal-ventral axis such that matrix dopamine levels are greater than striosome dopamine levels in the DS and vice versa in the VS. This idea is supported by recent findings concerning the heterogeneity of midbrain dopamine neurons and their various properties, including levels of activity and striatal projection fields (Ikemoto, 2007; Lammel et al., 2008). That is to say, it is possible that the dopamine neurons innervating striosomes are of a single type and thus the amount of evoked dopamine release is similar across striatal regions. In contrast, the matrix is innervated by multiple dopamine neuron subtypes with unique electrophysiological properties and striatal terminal fields. This is supported by findings that evoked dopamine release in the VS is less than in the DS (Calipari et al., 2012; Zhang et al., 2009a). Similarly, the loss of congruity between striosomal markers in the NAc (compared to the high degree of overlap in the dorsal striatum) is indicative of the much more heterogeneous structural and functional organization described by Gangarossa et al. (2013a) and may contribute to the regional heterogeneity in dopamine release observed in this study. Supporting this idea of a more complex NAc organization, a recent report by Kupchik et al. (2015) has called into question the direct/indirect pathway anatomical organization of the NAc.

Supporting one of our primary findings that dopamine release differs between striatal compartments, Brimblecombe and Cragg (2015) recently reported that substance P modulated dopamine release differently between dorsal striatal compartments and, with a *post hoc* comparison, that evoked dopamine release in the dorsal striatum differed between compartments. However, this report was limited to the dorsal striatum and did not examine any potential mechanisms underlying the compartment difference.

Altogether these findings may have numerous implications for the interpretation of previous studies. For example, the dopamine "hotspots" identified in the *in vivo* FSCV literature (May and Wightman, 1989; Moquin and Michael, 2009; Shu et al., 2013; Taylor et al., 2015) may correspond to striosome or matrix compartments, depending on the striatal region. Additionally, the "hotspot" differences in cocaine sensitivity or DAT inhibition described in the literature may be attributable to striosome/matrix compartment differences described in the current study (Cass et al., 1992; Cline et al., 1995; Glynn and Yamamoto, 1989; Mitch Taylor et al., 2012; Shu et al., 2014). Alternatively, the differences observed in these dopamine "hotspots" may be attributable to a confluence of factors including differences in dopamine terminal or dopamine neuron sensitivity to drugs of abuse (Covey et al., 2014).

The functional implications of these compartment differences have not been determined; however, a previous report examining intrastriatal electrical self-stimulation found that rats with stimulating electrodes contacting striosomes acquired self-stimulation behaviors more robustly than those with electrodes located in the matrix (White and Hiroi, 1998). Similarly, a recent report found that MORs in striosomes were critical in mediating the rewarding properties of an opiate drug (Cui et al., 2014). Together with reports demonstrating the effects of chronic psychostimulant administration on the induction of immediate early genes preferentially in striosomes (Biever et al., 2015; Canales and Graybiel, 2000; Capper-Loup et al., 2002; Gangarossa et al., 2013b; Jedynak et al., 2012; Saka et al., 2004; Vanderschuren et al., 2002), as well as, the more limbic nature of the striosome circuitry, a potential role for striosomes in the reinforcement of natural behaviors and drugs of abuse becomes apparent (Canales, 2005; Friedman et al., 2015).

In summary, using a transgenic mouse to *a priori* delineate striosome and matrix compartments of the dorsal and ventral striatum, we were able to demonstrate differences in evoked dopamine release between the striosome and matrix compartments that cannot be attributed to differences in dopamine D2 autoreceptor inhibition or nAChR modulation of dopamine release. We did, however, observe compartment differences in cocaine-enhanced dopamine levels and dopamine uptake inhibition that partially account for our observed results in the dorsal, but not ventral, striatum. These region and compartment differences in dopamine release and cocaine sensitivity may have broad implications on the interpretation of numerous published studies and should be considered in future studies of striatal dopamine and dopamine-dependent neurobiological processes and disorders.

Acknowledgments

References

Acevedo-Rodriguez A, Zhang L, Zhou F, Gong S, Gu H, De Biasi M, Zhou FM, Dani JA. Cocaine inhibition of nicotinic acetylcholine receptors influences dopamine release. Front Synaptic Neurosci. 2014; 6:19. [PubMed: 25237305]

Beier KT, Steinberg EE, DeLoach KE, Xie S, Miyamichi K, Schwarz L, Gao XJ, Kremer EJ, Malenka RC, Luo L. Circuit architecture of VTA dopamine neurons revealed by systematic input-output mapping. Cell. 2015; 162:622–634. [PubMed: 26232228]

Biever A, Puighermanal E, Nishi A, David A, Panciatici C, Longueville S, Xirodimas D, Gangarossa G, Meyuhas O, Herve D, Girault JA, Valjent E. PKA-dependent phosphorylation of ribosomal protein S6 does not correlate with translation efficiency in striatonigral and striatopallidal medium-sized spiny neurons. J Neurosci. 2015; 35:4113–4130. [PubMed: 25762659]

Brimblecombe KR, Cragg SJ. Substance P weights striatal dopamine transmission differently within the striosome-matrix axis. J Neurosci. 2015; 35:9017–9023. [PubMed: 26085627]

Cachope R, Mateo Y, Mathur BN, Irving J, Wang HL, Morales M, Lovinger DM, Cheer JF. Selective activation of cholinergic interneurons enhances accumbal phasic dopamine release: setting the tone for reward processing. Cell Rep. 2012; 2:33–41. [PubMed: 22840394]

Calipari ES, Huggins KN, Mathews TA, Jones SR. Conserved dorsal-ventral gradient of dopamine release and uptake rate in mice, rats and rhesus macaques. Neurochem Int. 2012; 61:986–991. [PubMed: 22819794]

Canales JJ. Stimulant-induced adaptations in neostriatal matrix and striosome systems: transiting from instrumental responding to habitual behavior in drug addiction. Neurobiol Learn Mem. 2005; 83:93–103. [PubMed: 15721792]

Canales JJ, Graybiel AM. A measure of striatal function predicts motor stereotypy. Nat Neurosci. 2000; 3:377–383. [PubMed: 10725928]

Capper-Loup C, Canales JJ, Kadaba N, Graybiel AM. Concurrent activation of dopamine D1 and D2 receptors is required to evoke neural and behavioral phenotypes of cocaine sensitization. J Neurosci. 2002; 22:6218–6227. [PubMed: 12122080]

Cass WA, Gerhardt GA, Mayfield RD, Curella P, Zahniser NR. Differences in dopamine clearance and diffusion in rat striatum and nucleus accumbens following systemic cocaine administration. J Neurochem. 1992; 59:259–266. [PubMed: 1613502]

Cline EJ, Adams CE, Larson GA, Gerhardt GA, Zahniser NR. Medial dorsal striatum is more sensitive than lateral dorsal striatum to cocaine inhibition of exogenous dopamine clearance: relation to [3H]mazindol binding, but not striosome/matrix. Exp Neurol. 1995; 134:135–149. [PubMed: 7672034]

Covey DP, Roitman MF, Garris PA. Illicit dopamine transients: reconciling actions of abused drugs. Trends Neurosci. 2014; 37:200–210. [PubMed: 24656971]

Cragg SJ, Rice ME. DAncing past the DAT at a DA synapse. Trends Neurosci. 2004; 27:270–277. [PubMed: 15111009]

Crittenden JR, Graybiel AM. Basal ganglia disorders associated with imbalances in the striatal striosome and matrix compartments. Front Neuroanat. 2011; 5:59. [PubMed: 21941467]

Crowley NA, Cody PA, Davis MI, Lovinger DM, Mateo Y. Chronic methylphenidate exposure during adolescence reduces striatal synaptic responses to ethanol. Eur J Neurosci. 2014; 39:548–556. [PubMed: 24236977]

Cui Y, Ostlund SB, James AS, Park CS, Ge W, Roberts KW, Mittal N, Murphy NP, Cepeda C, Kieffer BL, Levine MS, Jentsch JD, Walwyn WM, Sun YE, Evans CJ, Maidment NT, Yang XW. Targeted expression of mu-opioid receptors in a subset of striatal direct-pathway neurons restores opiate reward. Nat Neurosci. 2014; 17:254–261. [PubMed: 24413699]

Davis MI, Puhl HL 3rd. Nr4a1-eGFP is a marker of striosome-matrix architecture, development and activity in the extended striatum. PLoS One. 2011; 6:e16619. [PubMed: 21305052]

Eblen F, Graybiel AM. Highly restricted origin of prefrontal cortical inputs to striosomes in the macaque monkey. J Neurosci. 1995; 15:5999–6013. [PubMed: 7666184]

Friedman A, Homma D, Gibb LG, Amemori KI, Rubin SJ, Hood AS, Riad MH, Graybiel AM. A corticostriatal path targeting striosomes controls decision-making under conflict. Cell. 2015 Jun 4; 161(6):1320–1333. [PubMed: 26027737]

Fujiyama F, Sohn J, Nakano T, Furuta T, Nakamura KC, Matsuda W, Kaneko T. Exclusive and common targets of neostriatofugal projections of rat striosome neurons: a single neuron-tracing study using a viral vector. Eur J Neurosci. 2011; 33:668–677. [PubMed: 21314848]

Gangarossa G, Espallergues J, de Kerchove d'Exaerde A, El Mestikawy S, Gerfen CR, Herve D, Girault JA, Valjent E. Distribution and compartmental organization of GABAergic medium-sized spiny neurons in the mouse nucleus accumbens. Front Neural Circuits. 2013a; 7:22. [PubMed: 23423476]

Gangarossa G, Perroy J, Valjent E. Combinatorial topography and cell-type specific regulation of the ERK pathway by dopaminergic agonists in the mouse striatum. Brain Struct Funct. 2013b; 218:405–419. [PubMed: 22453353]

Gerfen CR. The neostriatal mosaic: compartmentalization of corticostriatal input and striatonigral output systems. Nature. 1984; 311:461–464. [PubMed: 6207434]

Gerfen CR, Engber TM, Mahan LC, Susel Z, Chase TN, Monsma FJ Jr, Sibley DR. D1 and D2 dopamine receptor-regulated gene expression of striatonigral and striatopallidal neurons. Science. 1990; 250:1429–1432. [PubMed: 2147780]

Gerfen CR, Herkenham M, Thibault J. The neostriatal mosaic: II. Patch- and matrix-directed mesostriatal dopaminergic and non-dopaminergic systems. J Neurosci. 1987; 7:3915–3934. [PubMed: 2891799]

Glynn GE, Yamamoto BK. In vivo neurochemical and anatomical heterogeneity of the dopamine uptake system in the rat caudate putamen. Brain Res. 1989; 481:235–241. [PubMed: 2524237]

Graybiel AM, Ragsdale CW Jr. Histochemically distinct compartments in the striatum of human, monkeys, and cat demonstrated by acetylthiocholinesterase staining. Proc Natl Acad Sci U S A. 1978; 75:5723–5726. [PubMed: 103101]

Herkenham M, Pert CB. Mosaic distribution of opiate receptors, parafascicular projections and acetylcholinesterase in rat striatum. Nature. 1981; 291:415–418. [PubMed: 6165892]

Ikemoto S. Dopamine reward circuitry: two projection systems from the ventral midbrain to the nucleus accumbens-olfactory tubercle complex. Brain Res Rev. 2007; 56:27–78. [PubMed: 17574681]

Jedynak JP, Cameron CM, Robinson TE. Repeated methamphetamine administration differentially alters fos expression in caudate-putamen patch and matrix compartments and nucleus accumbens. PLoS One. 2012; 7:e34227. [PubMed: 22514626]

Jimenez-Castellanos J, Graybiel AM. Subdivisions of the dopamine-containing A8-A9-A10 complex identified by their differential mesostriatal innervation of striosomes and extrastriosomal matrix. Neuroscience. 1987; 23:223–242. [PubMed: 3683862]

John, CE.; Jones, SR. Fast scan cyclic voltammetry of dopamine and serotonin in mouse brain slices. In: Michael, AC.; Borland, LM., editors. Electrochemical Methods for Neuroscience. Boca Raton (FL): 2007.

Johnston JG, Gerfen CR, Haber SN, van der Kooy D. Mechanisms of striatal pattern formation: conservation of mammalian compartmentalization. Brain Res Dev Brain Res. 1990; 57:93–102. [PubMed: 1965303]

Kemel ML, Desban M, Glowinski J, Gauchy C. Distinct presynaptic control of dopamine release in striosomal and matrix areas of the cat caudate nucleus. Proc Natl Acad Sci U S A. 1989; 86:9006–9010. [PubMed: 2813435]

Kemel ML, Desban M, Glowinski J, Gauchy C. Functional heterogeneity of the matrix compartment in the cat caudate nucleus as demonstrated by the cholinergic presynaptic regulation of dopamine release. Neuroscience. 1992; 50:597–610. [PubMed: 1359462]

Kincaid AE, Wilson CJ. Corticostriatal innervation of the patch and matrix in the rat neostriatum. J Comp Neurol. 1996; 374:578–592. [PubMed: 8910736]

Kupchik YM, Brown RM, Heinsbroek JA, Lobo MK, Schwartz DJ, Kalivas PW. Coding the direct/ indirect pathways by D1 and D2 receptors is not valid for accumbens projections. Nat Neurosci. 2015 Sep; 18(9):1230–1232. [PubMed: 26214370]

Lammel S, Hetzel A, Hackel O, Jones I, Liss B, Roeper J. Unique properties of mesoprefrontal neurons within a dual mesocorticolimbic dopamine system. Neuron. 2008; 57:760–773. [PubMed: 18341995]

Langer LF, Graybiel AM. Distinct nigrostriatal projection systems innervate striosomes and matrix in the primate striatum. Brain Res. 1989; 498:344–350. [PubMed: 2477114]

Levesque M, Parent A. The striatofugal fiber system in primates: a reevaluation of its organization based on single-axon tracing studies. Proc Natl Acad Sci U S A. 2005; 102:11888–11893. [PubMed: 16087877]

May LJ, Wightman RM. Heterogeneity of stimulated dopamine overflow within rat striatum as observed with in vivo voltammetry. Brain Res. 1989; 487:311–320. [PubMed: 2786444]

Mikula S, Parrish SK, Trimmer JS, Jones EG. Complete 3D visualization of primate striosomes by KChIP1 immunostaining. J Comp Neurol. 2009; 514:507–517. [PubMed: 19350670]

Mitch Taylor I, Jaquins-Gerstl A, Sesack SR, Michael AC. Domain-dependent effects of DAT inhibition in the rat dorsal striatum. J Neurochem. 2012; 122:283–294. [PubMed: 22548305]

Moquin KF, Michael AC. Tonic autoinhibition contributes to the heterogeneity of evoked dopamine release in the rat striatum. J Neurochem. 2009; 110:1491–1501. [PubMed: 19627437]

Prensa L, Parent A. The nigrostriatal pathway in the rat: a single-axon study of the relationship between dorsal and ventral tier nigral neurons and the striosome/matrix striatal compartments. J Neurosci. 2001; 21:7247–7260. [PubMed: 11549735]

Rice ME, Cragg SJ. Nicotine amplifies reward-related dopamine signals in striatum. Nat Neurosci. 2004; 7:583–584. [PubMed: 15146188]

Saka E, Goodrich C, Harlan P, Madras BK, Graybiel AM. Repetitive behaviors in monkeys are linked to specific striatal activation patterns. J Neurosci. 2004; 24:7557–7565. [PubMed: 15329403]

Shu Z, Taylor IM, Michael AC. The dopamine patchwork of the rat nucleus accumbens core. Eur J Neurosci. 2013; 38:3221–3229. [PubMed: 23937532]

Shu Z, Taylor IM, Walters SH, Michael AC. Region- and domain-dependent action of nomifensine. Eur J Neurosci. 2014; 40:2320–2328. [PubMed: 24766210]

Taylor IM, Nesbitt KM, Walters SH, Varner EL, Shu Z, Bartlow KM, Jaquins-Gerstl AS, Michael AC. Kinetic diversity of dopamine transmission in the dorsal striatum. J Neurochem. 2015; 133:522–531. [PubMed: 25683259]

Threlfell S, Lalic T, Platt NJ, Jennings KA, Deisseroth K, Cragg SJ. Striatal dopamine release is triggered by synchronized activity in cholinergic interneurons. Neuron. 2012; 75:58–64. [PubMed: 22794260]

Vanderschuren LJ, Schoffelmeer AN, Van Leeuwen SD, Hof L, Jonker AJ, Voorn P. Compartment-specific changes in striatal neuronal activity during expression of amphetamine sensitization are the result of drug hypersensitivity. Eur J Neurosci. 2002; 16:2462–2468. [PubMed: 12492441]

Venton BJ, Seipel AT, Phillips PE, Wetsel WC, Gitler D, Greengard P, Augustine GJ, Wightman RM. Cocaine increases dopamine release by mobilization of a synapsin-dependent reserve pool. J Neurosci. 2006; 26:3206–3209. [PubMed: 16554471]

Watabe-Uchida M, Zhu L, Ogawa SK, Vamanrao A, Uchida N. Whole-brain mapping of direct inputs to midbrain dopamine neurons. Neuron. 2012; 74:858–873. [PubMed: 22681690]

White NM, Hiroi N. Preferential localization of self-stimulation sites in striosomes/patches in the rat striatum. Proc Natl Acad Sci U S A. 1998; 95:6486–6491. [PubMed: 9600993]

Wu Q, Reith ME, Wightman RM, Kawagoe KT, Garris PA. Determination of release and uptake parameters from electrically evoked dopamine dynamics measured by real-time voltammetry. J Neurosci Methods. 2001; 112:119–133. [PubMed: 11716947]

Yorgason JT, Espana RA, Jones SR. Demon voltammetry and analysis software: analysis of cocaine-induced alterations in dopamine signaling using multiple kinetic measures. J Neurosci Methods. 2011; 202:158–164. [PubMed: 21392532]

Zhang L, Doyon WM, Clark JJ, Phillips PE, Dani JA. Controls of tonic and phasic dopamine transmission in the dorsal and ventral striatum. Mol Pharmacol. 2009a; 76:396–404. [PubMed: 19460877]

Zhang T, Zhang L, Liang Y, Siapas AG, Zhou FM, Dani JA. Dopamine signaling differences in the nucleus accumbens and dorsal striatum exploited by nicotine. J Neurosci. 2009b; 29:4035–4043. [PubMed: 19339599]
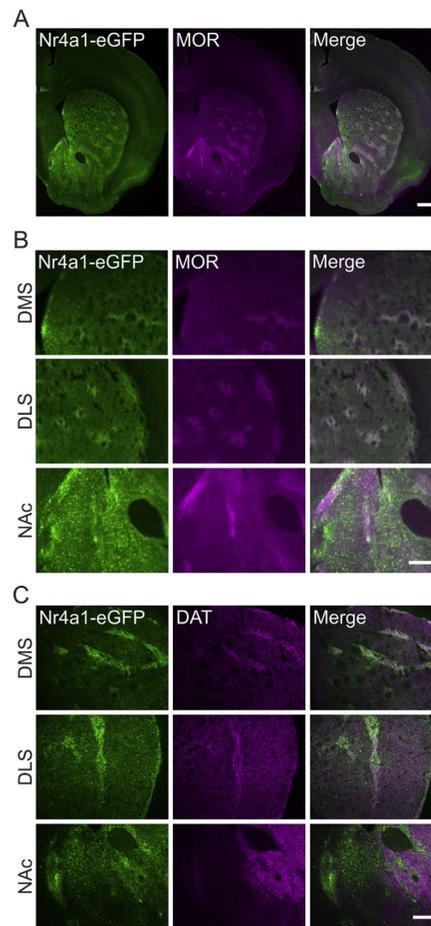
Fig. 1.
Nr4a1-eGFP and DAT are striosome-enriched. *A*, Nr4a1 is enriched in striosomes and colocalizes with MOR, a striosomal marker. Scale bar, 500 μm. *B*, Enlarged images from A to better show localization of Nr4a1-eGFP and MOR in the dorsomedial striatum (DMS), dorsolateral striatum (DLS), and Nucleus accumbens (NAc). Scale bar, 250 μm. *C*, Sample images demonstrating specificity of Nr4a1-eGFP and DAT colocalization in the DMS and DLS but not in the NAc. Scale bar, 250 μm.
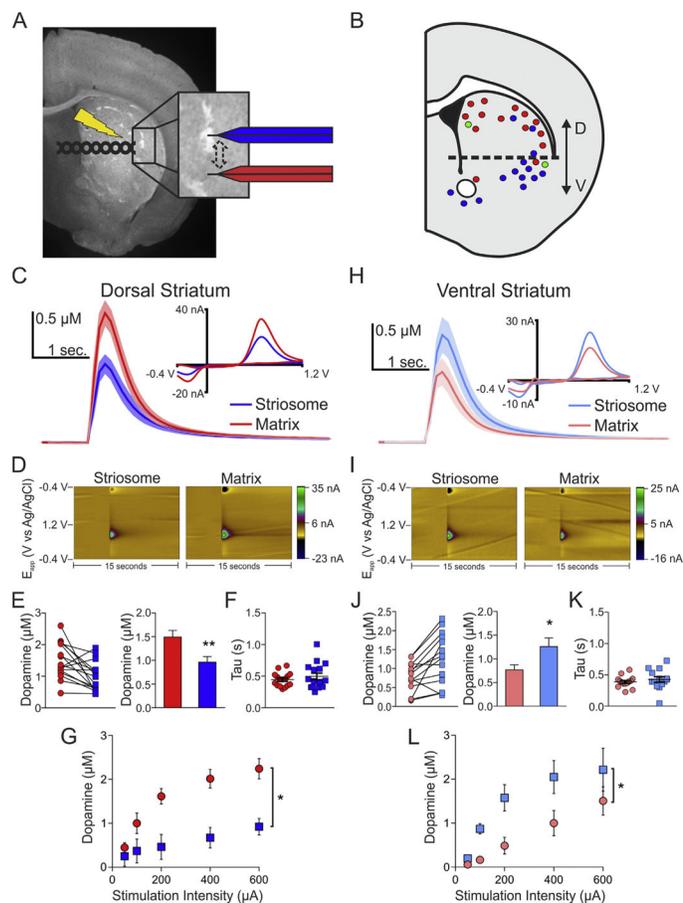
Fig. 2.
Dopamine release differs between striosomes and matrix in a region-dependent manner. *A*, Diagram of experimental configuration with an Nr4a1-eGFP slice. *B*, Approximate recording sites. Areas where striosome dopamine was more than or less than the corresponding matrix are represented by blue and red markers, respectively. Green markers represent no difference. *C*, Average dopamine transients for the striosome and matrix compartments in the dorsal striatum with representative CVs (inset). *D,* Corresponding color plots for dorsal striatum compartments depicting the voltammetric data with time on the X-axis, applied scan potential (E_{app}) on the Y-axis, and background-subtracted faradaic current on the Z-axis in pseudocolor. *E*, Calibrated data for individual dorsal striatum striosome-matrix pairs and summary bar graph. *F*, Dopamine transient decay rates (Tau) do not differ between compartments in the dorsal striatum. *G*, Input-Output curves examining the effect of stimulation intensity on dopamine release in the dorsal striatum. *H*, Average dopamine responses for the striosome and matrix compartments in the ventral striatum with representative CVs (inset). *I*, Corresponding color plots for ventral striatum compartments depicting the voltammetric data with time on the X-axis, applied scan potential (E_{app}) on the Y-axis, and background-subtracted faradaic current on the Z-axis in pseudocolor. *J*, Calibrated data for individual ventral striatum striosome-matrix pairs and summary bar graph. *K*, Dopamine transient decay rates (Tau) do not differ between compartments in the ventral striatum. *L*, Input-Output curves examining the effect of stimulation intensity on

dopamine release in the ventral striatum. *p < 0.05, **p < 0.01. Shaded areas and error bars represent the SEM. (For interpretation of the references to color in this figure legend, the reader is referred to the web version of this article.)
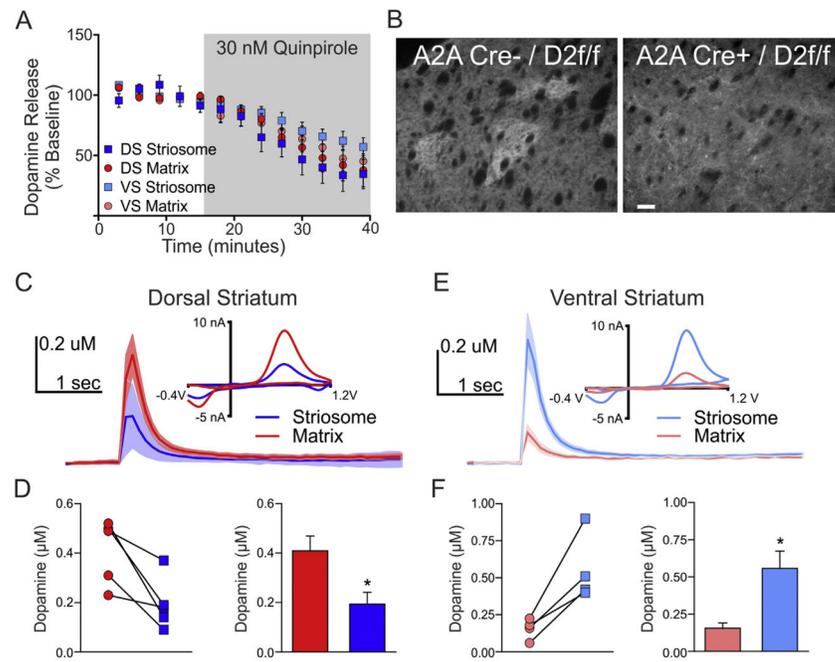
Fig. 3.
Inhibition of dopamine release by dopamine autoreceptor agonism is similar between compartments. *A*, Activation of dopamine D2 receptors also inhibited dopamine release equally in striosome and matrix compartments. *B*, Dopamine D2 receptor immunoreactivity is striosomal in D2$^{loxp/loxp}$ mice but not A2ACre/D2$^{loxp/loxp}$ mice. *C*, Average dopamine transients for the striosome and matrix compartments in the dorsal striatum with representative CVs (inset) in the presence of 30 nM quinpirole. *D*, Calibrated data for individual dorsal striatum striosome-matrix pairs and summary bar graph. *E*, Average dopamine transients for the striosome and matrix compartments in the ventral striatum with representative CVs (inset) in the presence of 30 nM quinpirole. *F*, Calibrated data for individual dorsal striatum striosome-matrix pairs and summary bar graph. Scale bar, 100 μm. Error bars represent the SEM.
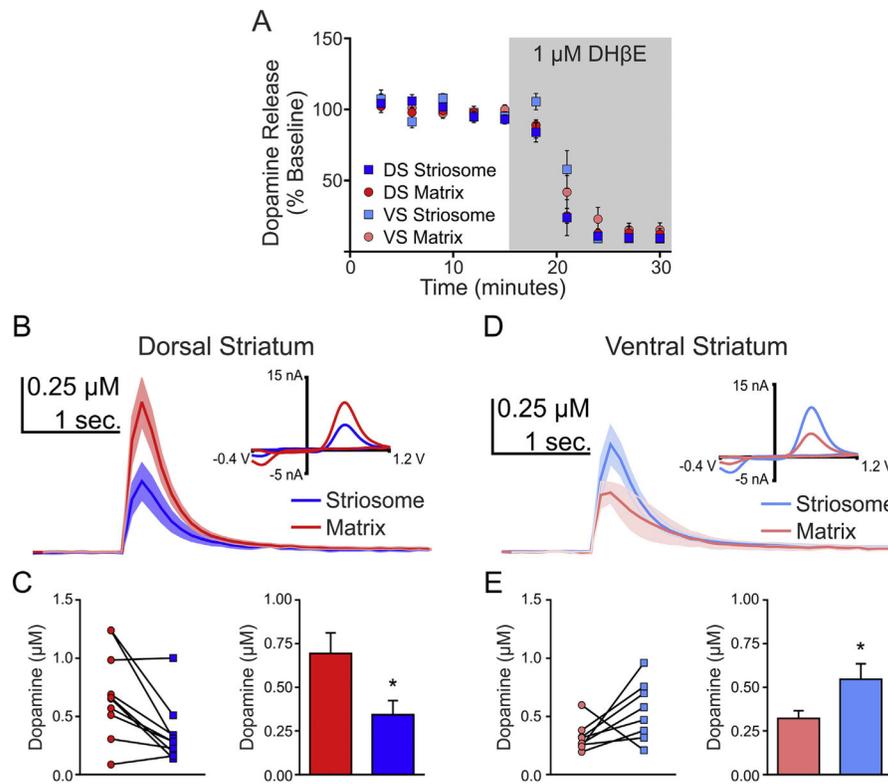
Fig. 4.
Compartment differences in dopamine release are not due to nAChRs. *A*, Inhibition of nAChRs by DHβE inhibited dopamine release equally in striosome and matrix compartments. *B*, Average dopamine transients in the presence of DHβE for the striosome and matrix compartments in the dorsal striatum with representative CVs (inset). *C*, Calibrated data for individual striosome-matrix pairs and summary bar graph. *D*, Average dopamine transients in the presence of DHβE for the striosome and matrix compartments in the ventral striatum with representative CVs (inset). *E*, Calibrated data for individual striosome-matrix pairs and summary bar graph. *p < 0.05. Error bars represent the SEM.

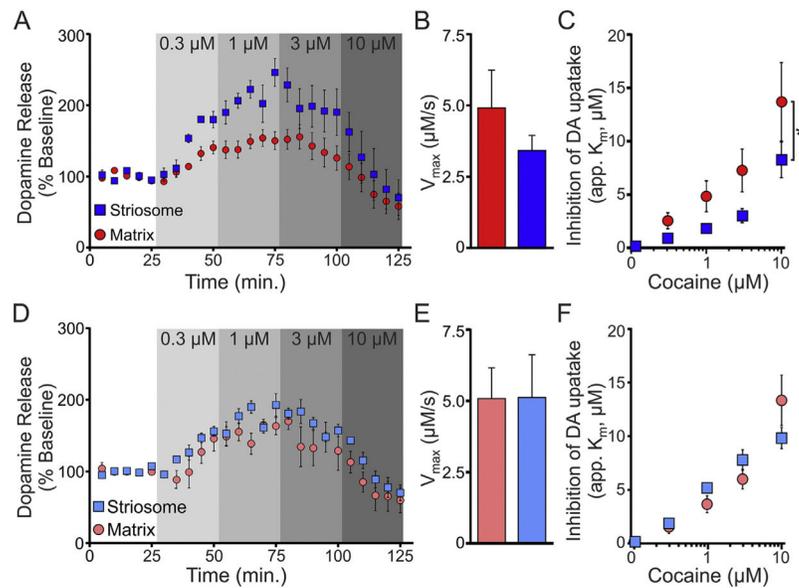**Fig. 5.**
Cocaine enhances dopamine detection and uptake inhibition differently between compartments in the dorsal striatum. ***A***, Cocaine concentration-response curves for dopamine release in striosome and matrix compartments of the dorsal striatum. ***B***, The maximal rates of dopamine uptake (V_{max}) did not differ between compartments. ***C***, Inhibition of dopamine uptake by cocaine was greater in the matrix than in the striosomes. ***D***, Average cocaine concentration-response curves for dopamine release in the striosome and matrix compartments of the ventral striatum. ***E***, The maximal rates of dopamine uptake (V_{max}) was similar between compartments. ***F***, Inhibition of dopamine uptake by cocaine was also similar between compartments in the ventral striatum. *$p < 0.05$. Error bars represent the SEM.